Materials and Design 193 (2020) 108848

Contents lists available at ScienceDirect

Materials and Design

journal homepage: www.elsevier.com/locate/matdes

Pulsed laser deposition of single phase n- and p-type Cu_2O thin films with low resistivity

Syed Farid Uddin Farhad [a,b,c,d,*], David Cherns [a], James A. Smith [b], Neil A Fox [a,b], David J. Fermín [c]

[a] H.H. Wills Physics Laboratory, School of Physics, University of Bristol, BS8 1TL, UK
[b] Diamond Laboratory, School of Chemistry, University of Bristol, BS8 1TS, UK
[c] Electrochemistry Laboratory, School of Chemistry, University of Bristol, BS8 1TS, UK
[d] Industrial Physics Division, BCSIR Laboratories, Bangladesh Council of Scientific and Industrial Research (BCSIR), Dhaka 1205, Bangladesh

HIGHLIGHTS

- Single phase n- and p-type Cu_2O thin films were achieved by controlling oxygen content in the PLD chamber.
- Donor and acceptor levels were estimated using Electrochemical Impedance and Optical data.
- Room temperature grown p-type Cu_2O films with resistivity ~23 mΩ·cm and Hall mobility ~4.8 cm^2/V.s.
- The n-type conductivities of Cu-O films were explained and attributed to the formation of electron-donating defect states.

GRAPHICAL ABSTRACT

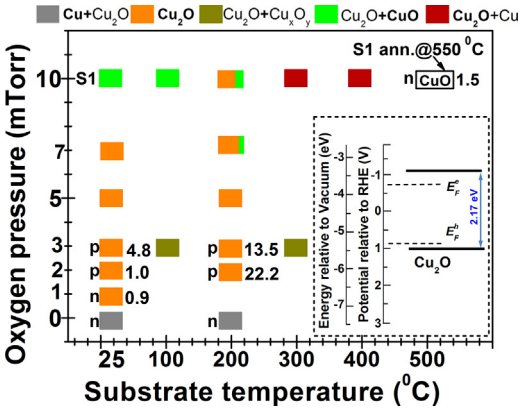

ARTICLE INFO

Article history:
Received 21 March 2020
Received in revised form 31 May 2020
Accepted 1 June 2020
Available online 05 June 2020

Keywords:
Pulsed laser deposition
Cuprous oxide (Cu_2O) thin film
P- and n-type conductivity
Hall coefficient measurement
Fermi level
Mott-Schottky analyses

ABSTRACT

Low resistivity (ρ ~ 3–24 mΩ·cm) with tunable n- and p-type single phase Cu_2O thin films have been grown by pulsed laser deposition at 25–200 °C by varying the background oxygen partial pressure (O_{2pp}). Capacitance data obtained by electrochemical impedance spectroscopy was used to determine the conductivity (n- or p-type), carrier density, and flat band potentials for samples grown on indium tin oxide (ITO) at 25 °C. The Hall mobility (μ_H) of the n- and p-type Cu_2O was estimated to be ~0.85 cm^2/V.s and ~ 4.78 cm^2/V.s respectively for samples grown on quartz substrate at 25 °C. An elevated substrate temperature ~ 200 °C with O_{2pp} = 2–3 mTorr yielded p-type Cu_2O films with six orders of magnitude higher resistivities in the range, ρ ~ 9–49 kΩ.cm and mobilities in the range, μ_H ~ 13.5–22.2 cm^2/V.s. UV–Vis-NIR diffuse reflectance spectroscopy showed optical bandgaps of Cu_2O films in the range of 1.76 to 2.15 eV depending on O_{2pp}. Thin films grown at oxygen rich conditions O_{2pp} ≥ 7 mTorr yielded mixed phase copper oxide irrespective of the substrate temperatures and upon air annealing at 550 °C for 1 h completely converted to CuO phase with n-type semiconducting properties (ρ ~ 12 Ω.cm, μ_H ~ 1.50 cm^2/V.s). The as-grown p- and n-type Cu_2O showed rectification and a photovoltaic response in solid junctions with n-ZnO and p-Si electrodes respectively. Our findings may create new opportunities for devising Cu_2O based junctions requiring low process temperatures.

* Corresponding author at: H.H. Wills Physics Laboratory, School of Physics, University of Bristol, BS8 1TL, UK
E-mail addresses: sf1878@my.bristol.ac.uk (S.F.U. Farhad), D.Cherns@bristol.ac.uk (D. Cherns), James.Smith@bristol.ac.uk (J.A. Smith), neil.fox@bristol.ac.uk (N.A. Fox), David.Fermin@bristol.ac.uk (D.J. Fermín).

https://doi.org/10.1016/j.matdes.2020.108848

1. Introduction

The semiconductor cuprous oxide (Cu_2O), has shown much promise in photocatalytic water splitting [1], resistive switching devices [2], thin film transistors (TFT) [3], gas sensors [4], as an anode material in Li-ion based batteries [5] and in photovoltaic (PV) applications [6]. It is non-toxic, earth-abundant, and could be prepared by physical and chemical methods [6–8]. In addition, single phase Cu_2O is desirable as an absorber material for solar cells because of its reported direct bandgap (E_g ~ 2.17 eV) and high absorption coefficient (above 10^5 cm^{-1}) in the visible region of solar radiation and, potentially, the ability to dope both n- and p-type via manipulating processing conditions [9–15]. The natural p-type conductivity of Cu_2O is believed to stem from copper vacancies (V_{Cu}) in the crystal lattice [16,17], and its suitable band alignment with other wide bandgap n-type metal oxide semiconductors, such as ZnO [18,19] and TiO_2 [20,21], makes it attractive for realizing reasonably efficient heterojunction solar cells. In contrast, the origin of intrinsic n-type conductivity is a matter of debate [9,22,23], yet it has gained substantial interest because of the possibility of the formation of homojunction solar cells [7,9,12,14,24] to suppress the deleterious interfacial defects states often formed in the case of most heterojunction solar cells ([25] and refs. therein). The oxygen vacancy (V_o) [11] and copper interstitial (Cu_i) defects in Cu_2O lattice have been proposed for the electron-donating source in explaining the experimental results ([22] and refs. therein). However, the formation energy of V_o is relatively low compared to that of Cu_i irrespective of the copper-rich (poor)/oxygen-poor (rich) growth conditions [22]. In general, the donor- and acceptor- levels should be shallow for effective n- and p-type semiconductors. Carrier concentrations over of ~10^{16} cm^{-3} and mobilities at least ~5 cm^2/V.s are also necessary for efficient Cu_2O based optoelectronic devices [11,26,27]. In the case of intrinsic n-type Cu_2O, most of the experimental works reported deep donor levels ([22] and refs. therein), therefore, unlikely to overcome the native p-type conductivity stemming from cation deficiency (V_{Cu}) [6] due to self-compensation [28]. However, a recent report by Nandy et al. demonstrated that controlling the oxygen vacancies (V_o) into the Cu_2O crystal (i.e., $Cu_2O_{1-\delta}$) may induce an impurity state close to the conduction band thereby enhancing the electron-donating ability due to the unshared d-electrons of Cu atoms (nearest to the vacancy site) [29]. Their theoretical approach further suggested that the formation energy for obtaining 2.08% ($\delta = 0.208$) of V_o in Cu_2O could be as low as 0.32 eV under oxygen deficient condition, suggesting that the stable $Cu_2O_{1-\delta}$ entity maybe experimentally viable [29].

Several physical [6,25,30–32] and wet-chemical [3,5,15,33–36] based deposition methods have been employed to produce phase pure Cu_2O. Among them, pulsed laser deposition (PLD) offers good control on a wide range of processing parameters such as laser wavelength, pulse repetition rate, laser energy per pulse (LP), background gas pressure (O_{2pp}), substrate temperature (T_{sub}) etc. and has been demonstrated to give single phase cuprous oxides with good structural, morphological and electrical properties [11,25,27,37,38]. Previous work [25,37] demonstrated the similar microstructures of Cu_xO_y (a defect variant of the basic-Cu_2O) thin films on various substrates using different PLD processing conditions; these identified favorable process conditions within which we now focus. These investigations, on the effect of T_{sub} (≤400 °C) and O_{2pp}(≤10 mTorr), achieve single phase Cu_2O with varying optical and electrical properties by exploiting the non-equilibrium deposition environment of PLD. The ablation species react with ambient background gas chemically and physically while it proceeds towards the substrate from the target and affects the resulting film properties. Oxygen content in copper oxide films can be adjusted through controlling the oxygen partial pressure (O_{2pp}) during growth. In the literature most of the investigations related to electrical properties of Cu-O films deal with films deposited under oxygen rich conditions near the Cu_2O/CuO boundary. There is less information for films deposited at the Cu/Cu_2O boundary, where an n-type Cu_2O may exist [39] due to the predominant presence of oxygen vacancy (V_o) as opposed to the hole creating copper vacancy (V_{cu}). Meyer et al. [6], roughly estimated the binding energy of donor and acceptors for Cu_2O to be 266 meV and 156 meV using effective mass theory (EMT) and discussed that carrier densities well above ~10^{18} cm^{-3} are necessary to overcome natural p-type conductivity due to the cation vacancy (V_{cu}). Wang et al. [40] argued that n-type conductivity of Cu_2O is possible only if the V_o would exist at very high concentrations synthesized in oxygen poor conditions. In our previous report we demonstrated the n-type conductivity of Cu_2O based on electrochemical Mott-Schottky analyses for the samples grown by PLD at room temperature with oxygen poor condition ($O_{2pp} << 1$ mTorr) [41]. Recently, Xu et al. [11], also reported PLD grown phase pure Cu_2O films produced at 600 °C under oxygen poor conditions ($O_{2pp} = 0.09$ Pa ≈ 0.68 mTorr). The films exhibited p-type conductivity and upon post N_2 plasma treatment of the as-deposited samples they observed a phase transition from pure Cu_2O to a mixture of Cu_2O and Cu with an accompanied change from p to n-type conduction. Therefore, in this work, the effects of O_{2pp} (both oxygen-rich and oxygen-poor conditions) in controlling composition, microstructure, optical, electrical, and electrochemical impedance properties of PLD Cu_2O films were investigated. We found that under suitable deposition conditions both n- and p-type copper oxide thin films can be realized which are discussed below.

2. Experimental methods

2.1. Growth of PLD films

A simple PLD setup using a UV-ArF Excimer Laser (wavelength: 193 nm, repetition rate: 10 Hz, pulsed width: 20 ns, spot size: ~1 mm^2, energy (LP): 25 ± 4 mJ/pulse) was used to deposit copper oxide thin films on amorphous quartz, polycrystalline ITO, and single crystalline NaCl(100) substrates under the following conditions: Base vacuum of the PLD chamber ≤10^{-5} Torr; oxygen partial pressure (O_{2pp}): 0–10 mTorr; target-substrate distance ~5 cm; substrate temperature (T_{sub}): ranging from non-intentionally heated (RT ~ 25 °C) – 400 °C. The substrate temperature was controlled by halogen bulb heater and measured by using a digital thermocouple as described in ref. [25]. The substrate temperature and oxygen partial pressure were varied to allow the film to grow in a stable regime, where no decomposition of the film was observed. Post annealing treatment was also given to some of the as-grown Cu_2O films under controlled O_2 ambient inside the PLD chamber for comparison purposes.

Prior to film deposition, all substrates were ultrasonically cleaned successively in Toluene, Acetone, isopropanol and ultra-pure water (Mili-Q, 18 MΩ·cm) for 15 min followed by an Ar blown dry. All substrates were subjected to an UV-Ozone clean for 20 min immediately before being mounted in the PLD chamber. The target material was commercially available hot pressed ceramic Cu_2O (purity~99.95%). The target was ablated for 5 min prior to actual deposition on the substrates.

2.2. Characterization of PLD samples

The X-ray Diffraction (XRD) spectra were recorded with Bruker AXS D8 Advance powder X-ray diffractometer using Cu K_α($\lambda = 1.5406$ Å) radiation. The diffraction patterns were recorded with a step size of ~0.025^0 and a time per step of 18 s, the samples were rotated to homogenize the measurements. TEM analyses of samples grown on NaCl(100) were investigated by a JEOL 2010 and a Philips EM 430 as described in ref. [25] where the TEM camera length calibration procedure was also discussed. Raman and Photoluminescence spectra were recorded at room temperature in the backscattering geometry with a Renishaw 2000 confocal spectrometer using $\lambda_{ext} = 514.5$ nm Ar-ion laser ($P \leq 5$ mW) as an excitation source. The optical transmission and diffuse reflection measurements of films deposited on quartz substrate were made using a UV-VIS-NIR spectrophotometer (Shimadzu UV2600

plus) coupled with an integrating sphere. Sheet resistance was measured by a Keithley 2400 source-measure-unit (SMU) coupled with a custom made collinear 4-point probe. Measurements of highly resistive films (>200 MΩ) were carried out using a precision current source (Keithley 6221 AC/DC) coupled with a Nanovoltmeter (Keithley 2182A). To minimize the non-uniformity nature of the PLD thin film, measurements were performed over three or more different areas of the sample to get a final resistance value. Thicknesses of the PLD films were estimated by combined analyses of FE-SEM (JEOL JSM 6330F) cross-sectional imaging and Variable Angle Spectroscopic Ellipsometry (VASE) (M-2000 U, J.A. Woollam Co.) [37]. Hall mobilities of samples grown on quartz were measured as accurately as possible using a home-made Hall coefficient measurement setup utilizing a commercial 1 Tesla permanent magnet (Magnetsales UK Ltd.) with gold coated electrical contact pads in the van der Pauw sample configuration (see supplementary materials for details). Both Cyclic Voltammetry (CV) and Electrochemical Impedance Spectroscopy (EIS) measurements were performed under dark conditions using a Potentiostat (Autolab, PGSTAT-30) equipped with a frequency analyzer. An AC signal of 20 mV amplitude with frequencies ranging from 50 Hz to 10 kHz was applied at a set of constant bias voltage over a narrow potential window to preserve the stability of the Cu_2O film. The Keithley SMU coupled with a homemade multiprobe workstation was also used to measure I-V curve of the Cu_2O-based solid p-n junctions.

3. Results and discussion

Four sets of samples were deposited in an attempt to grow high quality single phase copper (I) oxide (Cu_2O) at relatively low temperatures with a range of conductivities. In the first two sets of samples, substrate temperature was varied from 25 °C (RT) to 400 °C with two different constant oxygen partial pressure(O_{2pp}), namely 3 mTorr and 10 mTorr, in order to find out the optimum process conditions for single phase copper oxide. In the other two sets, the oxygen content inside the PLD chamber was varied ($0 \le O_{2pp} \le 7$ mTorr) at two substrate temperatures (T_{sub}), 25 °C and 200 °C. The PLD thin films grown at 25 °C $\le T_{sub} \le$ 400 °C with constant $O_{2pp} \approx 10$ mTorr were found to be mainly composed of a mixture of Cu_2O and more O-rich Cu-O phases as evident from the XRD analyses (see Fig. S1a for details). Therefore, the oxygen rich ($O_{2pp} = 10$ mTorr) samples will not be considered further in the discussion below. As a quick guide for the readers: the structural, compositional, and electrical characteristics of samples investigated are summarized in Fig. 1.

The microstructure and surface morphology of Cu (I) oxide thin films are seemingly independent of substrate material as investigated by XRD and FE-SEM where all films are polycrystalline in nature showing grain sizes in the range 50 nm to 150 nm, but with some larger grains and texture on crystalline substrates (see Fig. S1.1 and Fig. S5.1 to S5.4 in supplementary material).

It can be seen from Fig. 1 (Green, brown, and mixed colored squares) that elevated T_{sub} and high level $O_{2pp} \ge 7$ mTorr produced a mixture of Cu-O phases evident from XRD and Raman analyses (shown in Fig. S1-S2 in supplementary materials). In contrast, substrate temperature 100 °C and 300 °C with fixed $O_{2pp} = 3$ mTorr produce non-stoichiometric Cu (I) oxide ($Cu_2O + Cu_xO_y$) exhibiting cubic SAED patterns similar to phase pure polycrystalline Cu_2O (see also Fig. S1b). The origin of the Cu_xO_y phase - a defect structure of Cu_2O - was discussed in detail in our previous report [25]. It should be noted that depositing films at $T_{sub} = 25$ °C and $T_{sub} = 200$ °C while tuning the O_{2pp} allows one to achieve single phase Cu_2O with varying electrical properties (see orange color squares and numerical value for carrier mobility in Fig. 1). The structural properties of these films are presented in Fig. 2 below.

Fig. 2a and 2b show the XRD profiles of as-grown films deposited at $T_{sub} = 25$ °C (RT-grown) and $T_{sub} = 200$ °C (HT-grown), respectively, on quartz substrates with varying O_{2pp}. XRD results revealed that single phase Cu_2O, with no contribution from Cu and CuO, could be produced with 1 mTorr $\le O_{2pp} \le$ 7 mTorr in the case of RT-grown and with 3 mTorr $\le O_{2pp} \le$ 5 mTorr in the case of HT-grown thin films. In these phase purity limits, both RT- and HT-grown mainly exhibit $Cu_2O(111)$ and $Cu_2O(200)$ Bragg peaks but the former displays an additional $Cu_2O(110)$ peak at $2\theta \approx 29.5^0$. Metallic Cu inclusions were observed in the RT-grown film with $O_{2pp} < 1$ mTorr and in the HT-grown film with $O_{2pp} \le 2$ mTorr presumably due to the deficiency of oxygen species in the PLD chamber. However, RT-grown film with $O_{2pp} = 1$ mTorr show single phase Cu_2O films evident from XRD and SAED pattern (see Fig. 2a and Fig. 1a). Both RT- and HT-grown films with $O_{2pp} > 7$ mTorr were found to be mixed Cu-O phase (see Fig. S2) with CuO as a major product. Notice also that RT- and HT-grown films approached towards strong {100} and {111} texturing, respectively, with increasing O_{2pp} up to 7 mTorr (see also Fig. S3a). The average crystallite domain size estimated by using Scherrer formula was found to be in the range 5–15 nm and found to be following a decreasing trend with increasing O_{2pp} (for details see fig. S3b) most probably due to the inclusion of oxygen rich Cu-O phase at higher O_{2pp} [37]. However, up to $O_{2pp} = 5$ mTorr, PLD grown thin films are composed of Cu(I) oxide as evident from the SAED patterns shown in Fig. 2c and 2d. The arced SAED patterns, more conspicuous in Fig. 2d, is due to the micro-twinning on , , and planes while viewed down the [011] zone axis [25].

Room temperature Raman analyses have also been conducted to supplement the XRD results in order to further confirm the phase purity of RT-grown and at HT-grown samples deposited with 2 mTorr $\le O_{2pp} \le$ 7 mTorr which are presented in Fig. 3 below. All Raman peaks in both groups of samples can be assigned with reported phonon modes of Cu_2O crystal only (solid lines) [25], except for the HT-grown with $O_{2pp} = 7$ mTorr film which is seen to be a mixture of Cu_2O (solid lines) and CuO (dotted lines) (cf. Fig. 3a and Fig. 3b). The presence of CuO phase is confirmed by the additional presence of A_g and $B_g^{(1)}$ modes at ~296 cm^{-1} and ~ 346 cm^{-1} respectively (see top panel in Fig. 3b). The position of Raman peaks for copper oxide compounds vary considerably in literature, but the vibrational modes for all three copper oxide phases cited in references [6, 25, 42] clearly indicate that none of the Raman signals in Fig. 3 (up to $O_{2pp} \approx 5$ mTorr in the case of HT-grown films) are related to CuO and/or Cu_4O_3 phases.

The room temperature Photoluminescence (RT-PL) of thin films grown at $T_{sub} \approx 25$ °C(RT) and $T_{sub} \approx 200$ °C(HT) with 2 mTorr $\le O_{2pp} \le$ 5 mTorr including Cu_2O PLD target are shown in Fig. 4. All luminescence peaks (solid lines) can be attributed to copper oxide phases, consistent with the results reported previously [25]. The exciton-related (X_0 - Γ_{12}^-) emission peak is clearly seen in the RT-PL spectrum for all PLD films including the target material suggesting good quality Cu_2O thin films irrespective of O_{2pp} conditions. The luminescence peaks centering at ~760 nm and ~ 880 nm have been put forward for Cu_3O_2 and [V_{Cu}^- - V_O^+] complex respectively [25]. Notice that at low $O_{2pp} = 2$–3 mTorr, HT-grown films showed an enhanced (X_0 - Γ_{12}^-) peak with additional [V_{Cu}^- - V_O^+] complex peak which is not conspicuous in RT-grown films. These samples also exhibited diminished V_{cu} peak (see Fig. 4b).

The optical bandgap of the RT- and HT- samples grown with O_{2pp} up to 7 mTorr were estimated by Tauc plot generated from diffuse reflection data using K-M function [43] and shown in Fig. 5. The bandgaps (E_g) for RT-grown Cu_2O thin films are found to be gradually and consistently increasing approximately from 1.76 eV to 2.15 eV with increasing O_{2pp} from 1 to 7 mTorr (see Fig. 5a). In contrast, for HT-grown samples, E_g is found to reach a maximum ~2.05 eV for O_{2pp} of 5 mTorr and then to decrease for higher O_{2pp} (see Fig. 5b). The optical band gap thus approaches the bandgap value of bulk Cu_2O ($E_g = 2.17$ eV), and presumably therefore stoichiometric phase formation, at optimum values of O_{2pp}. The lowest measured optical bandgap (~1.65 eV) of HT-grown $O_{2pp} = 7$ mTorr film suggests an oxygen rich Cu-O phase as also evident from its Raman spectrum (see top panel in Fig. 3b). The RT-grown sample (S1) annealed in air at 550 °C for 1 h also exhibited a lower optical

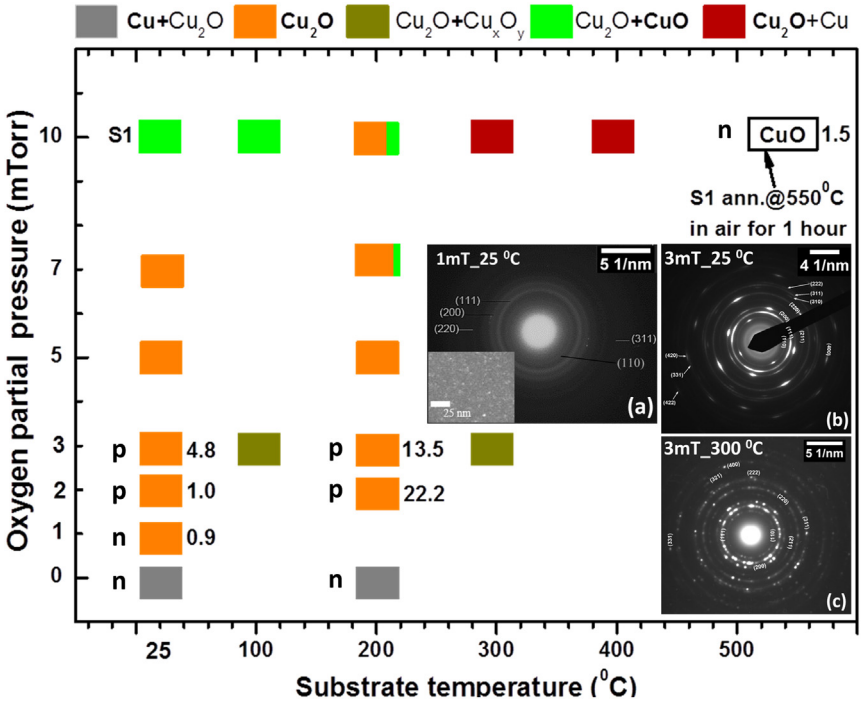

Fig. 1. (color online) Deposition diagram of PLD grown copper oxide phases with varying O_{2pp} and T_{sub}. The colored squares represent the different phase compositions shown at the top of the graph. The carrier mobility of some as-deposited and annealed S1(Cu(II) oxide: CuO) films are also included in the analysis for comparison purposes. SAED patterns of samples grown on NaCl (100) with (a) O_{2pp} = 1 mTorr_T_{sub} = 25 °C (Inset: bright field image), (b) O_{2pp} = 3 mTorr_T_{sub} = 25 °C, and (c) O_{2pp} = 3 mTorr_T_{sub} = 300 °C are showing single phase Cu (I) oxide with different morphologies.

bandgap ~1.45 eV due to complete conversion to CuO (see Fig. S4 in supplementary material). The lower optical bandgap for films with low O_{2pp}, suggest oxygen vacancies (V_o) which introduce defect states in the bandgap leading to a lower effective bandgap compared to the stoichiometric Cu_2O.

Fig. 6 (below) shows the four point collinear probe measured electrical resistivity of RT- and HT-grown films as a function of O_{2pp}. The data points for the films grown without O_2 injection in the PLD chamber have also been included in the analyses for the sake of completeness and comparison.

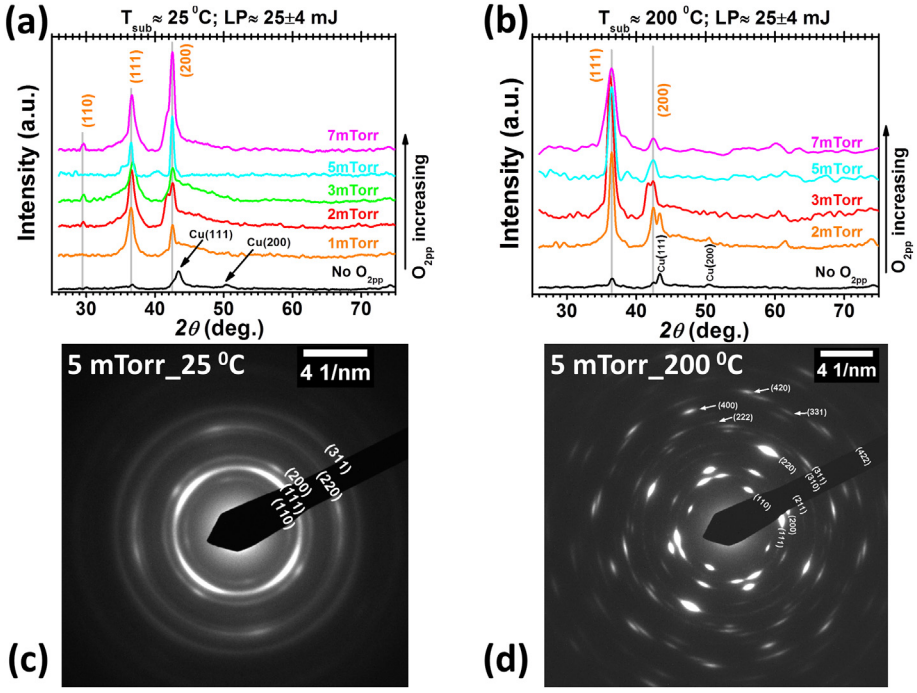

Fig. 2. (color online) PLD grown copper oxide thin films deposited at various O_{2pp} at two constant substrate temperatures: XRD patterns of Cu_2O films deposited on quartz glass at (a) T_{sub} = 25 °C and (b) T_{sub} = 200 °C as a function of O_{2pp}. Vertical lines (faint) represent the Bragg's reflection lines for bulk Cu_2O. SAED pattern of samples grown on NaCl(100) at T_{sub} = 25 °C (c) and T_{sub} = 200 °C (d) with a constant O_{2pp} = 5 mTorr. The rings/spots are indexed to assist the reader.

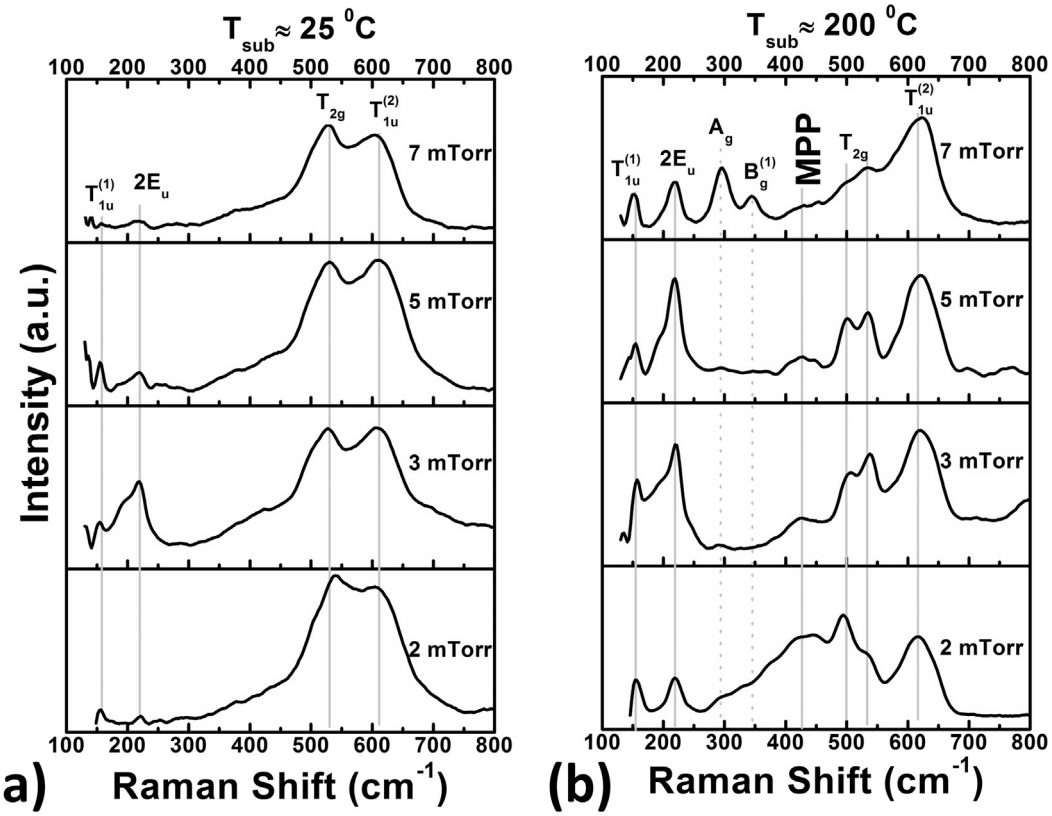

Fig. 3. Room temperature Raman spectra of, as-grown copper oxide thin films on quartz glass as a function of O_{2pp} at $T_{sub} \approx 25$ °C (a), and at $T_{sub} \approx 200$ °C (b). Vertical lines represent the reference vibrational mode of copper oxide.

As can be seen from the Fig. 6a, the resistivities of RT-grown films are found to be monotonically increasing with increasing O_{2pp}. At 1 mTorr ≤ O_{2pp} ≤ 3 mTorr PLD ambient their resistivities were estimated to be roughly 3–24 mΩ·cm which is ~3 orders of magnitude lower than the reported resistivity (40–60 Ω·cm) for Cu_2O films grown by PLD above $T_{sub} \geq 600$ °C [44]. On the other hand, the resistivities of RT-films with 5 mTorr ≤ O_{2pp} ≤ 7 mTorr PLD ambient are quite high, roughly in the range 20–38 kΩ·cm (see Fig. 6a) due to more stoichiometric Cu_2O phase formed in the oxygen rich conditions. In contrast, the resistivity of HT-grown films without injecting O_2 into the PLD chamber was estimated to be below 7 mΩ·cm (see Fig. 6b). The HT-grown film deposited using $O_{2pp} = 2$ mTorr exhibited the highest resistivity of ~49 kΩ·cm among all samples, due to inclusion of metallic Cu into the Cu_2O matrix which compensates available holes leading to insulating thin films.

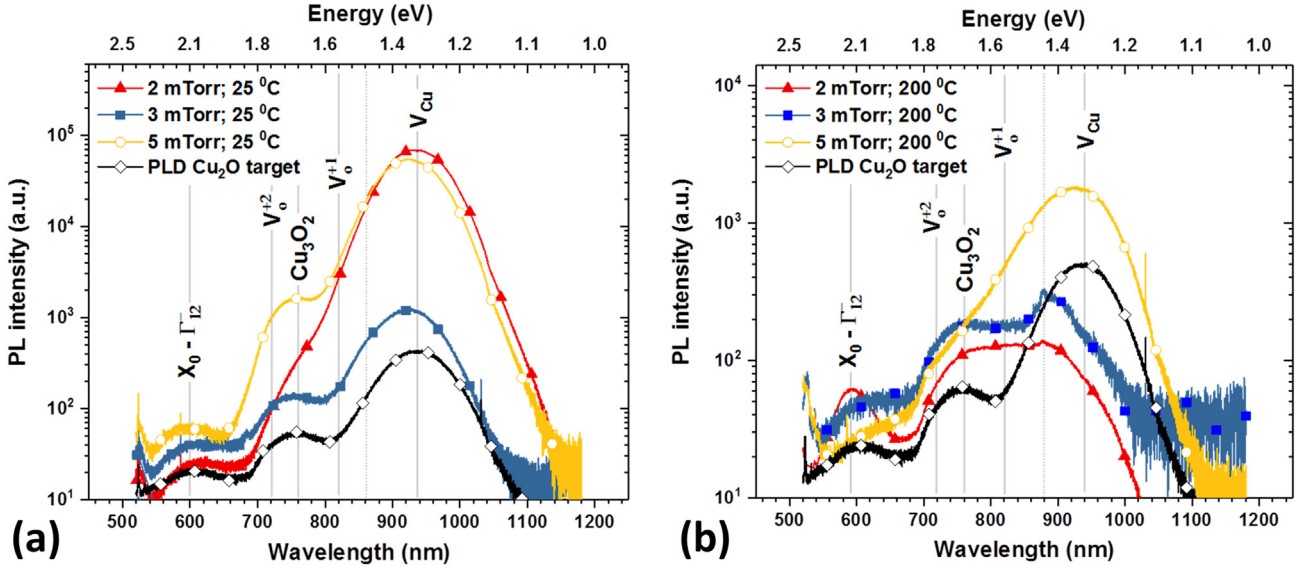

Fig. 4. (color online) Room temperature photoluminescence spectra of, as grown copper oxide thin films onto quartz glass as a function of O_{2pp} at $T_{sub} \approx 25$ °C (a), and at $T_{sub} \approx 200$ °C (b). Vertical lines represent the luminescence bands of cuprous oxide.

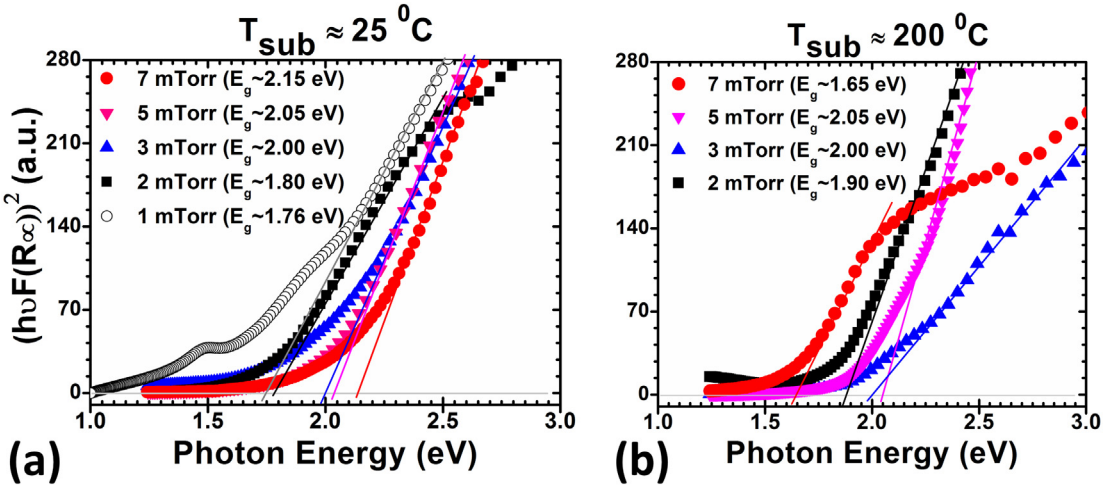

Fig. 5. (color online) Comparison of modified Tauc plot of as-grown copper oxide thin films onto quartz glass as a function of O_{2pp} deposited at $T_{sub} \approx 25$ °C (a), and at $T_{sub} \approx 200$ °C (b).

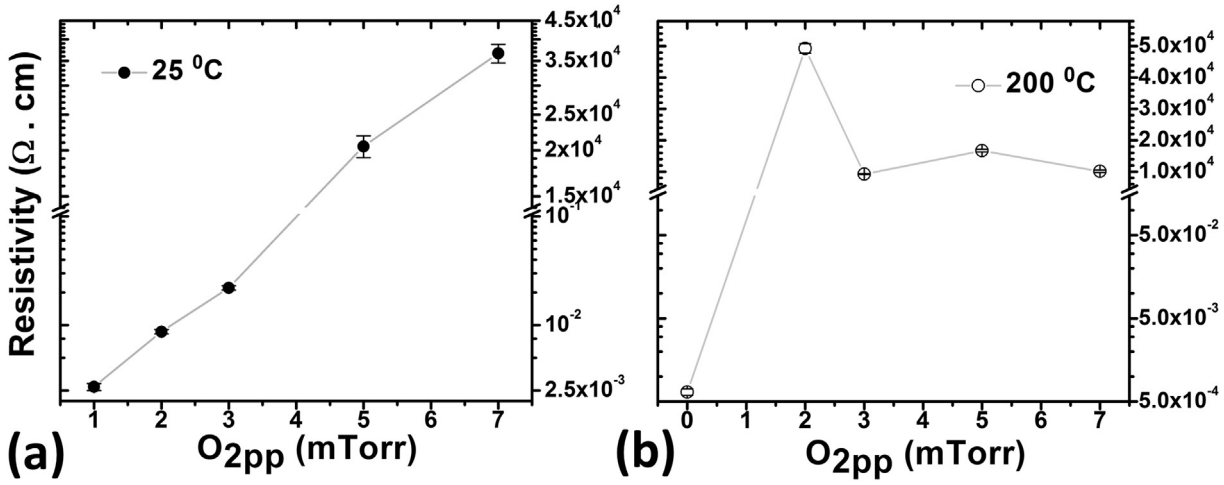

Fig. 6. Variation of Electrical resistivity of as-grown copper oxide thin films onto quartz glass as a function of O_{2pp} deposited at $T_{sub} \approx 25$ °C (a) and $T_{sub} \approx 200$ °C (b).

Since, the PLD chamber provides highly non-equilibrium growth environment to the energetic ablated particles and therefore, the probability to exist metallic Cu as ionized defect states (Cu_i^+) is very high in oxygen poor heated substrate surface. These energetic Cu_i^+ defects compensate available holes leading to insulating thin films compared to the films grown in oxygen rich conditions. Similar observation was reported by X. Liu et al. for PLD grown Cu_2O ($T_{sub} = 600$ °C on MgO(110)) with varying O_{2pp} [26]. In fact, the resistivities of 2 mTorr ≤ O_{2pp} ≤ 7 mTorr HT-grown films are roughly six orders of magnitude higher than that of the film grown without oxygen. These results are also suggesting that oxygen rich PLD ambient leads to more stoichiometric copper oxide, thereby resulting in more insulating thin films due to the lack of charge carrier creating defect (vacancy type) concentrations.

Hall coefficient measurements and Mott-Schottky plots (see Fig. 7a) constructed from electrochemical impedance spectra [9,33] were also carried out for samples grown with identical deposition PLD conditions on quartz and ITO substrates respectively (see Fig. S7 in supplementary material). The results together with optical bandgap values are summarized in Table 1. As can be seen, samples grown with $O_{2pp} = 2$–3 mTorr, showed a p-type conductivity with appreciable Hall mobility (μ_H) ~ 4.78 ± 0.01 cm^2/V.s and ~ 22.20 ± 0.01 cm^2/V.s respectively in RT- and HT-grown PLD Cu_2O films. The higher mobility in HT-grown PLD films could be attributed to the better crystalline and optoelectronic quality evident from XRD, SAED, Raman, and RT-PL analyses. However, the lower carrier concentrations (~ $6 \times 10^{12-13}$ cm^{-3}) of HT-grown films may be attributed to the hole killing [V_{Cu}^- - V_O^+] defect complex seen in PL spectra (see Fig. 4b).

The acceptor concentration, N_a ~ $6 \times 10^{12-13}$ cm^{-3} and mobility, μ_H ~ 13–22 cm^2/V.s estimated for $T_{sub} \approx 200$ °C(HT) samples are consistent with previous results [6]. The high mobility indicates that PLD films grown at 200 °C possess reasonably good electrical quality, however, a carrier concentration as high as ~10^{14}–10^{16} cm^{-3} is desirable for potential Cu_2O based device applications [27]. Therefore, for some specific device applications [3,26,45] RT-grown PLD Cu_2O may be utilized.

Notice that carrier density in RT-grown samples is exceptionally high compared to that of HT-grown samples. For example, with $O_{2pp} = 2$ mTorr, carrier density ~ $(5.71 \pm 0.18) \times 10^{12}$ cm^{-3} obtained for HT-grown sample is at least eight orders of magnitude lower than the carrier density ~ $(6.97 \pm 0.01) \times 10^{20}$ cm^{-3} for RT-grown samples. With increasing O_{2pp} content slightly to 3 mTorr for RT-grown sample, it was obtained as ~$(5.45 \pm 0.23) \times 10^{19}$ cm^{-3} which is still roughly six orders of magnitude higher than its HT-grown counterpart. The effective density of states ($D(E_f)$) for these samples are in the range ($D(E_f)$) ~ 1.35–5.67 × 10^{21} $(eV)^{-1}$ cm^{-3} estimated from EIS data by a similar approach presented in ref. [46] using the equation: $D(E_f) = (C_{sc})^2/[\varepsilon_0 \varepsilon . e^2]$, where, C_{sc} is the space charge capacitance, ε_0 is permittivity of free space (8.854×10^{-12} $F.m^{-1}$), ε is the relative dielectric constant (~6.6 for Cu_2O [33]) and e is the electronic charge (see supplemental

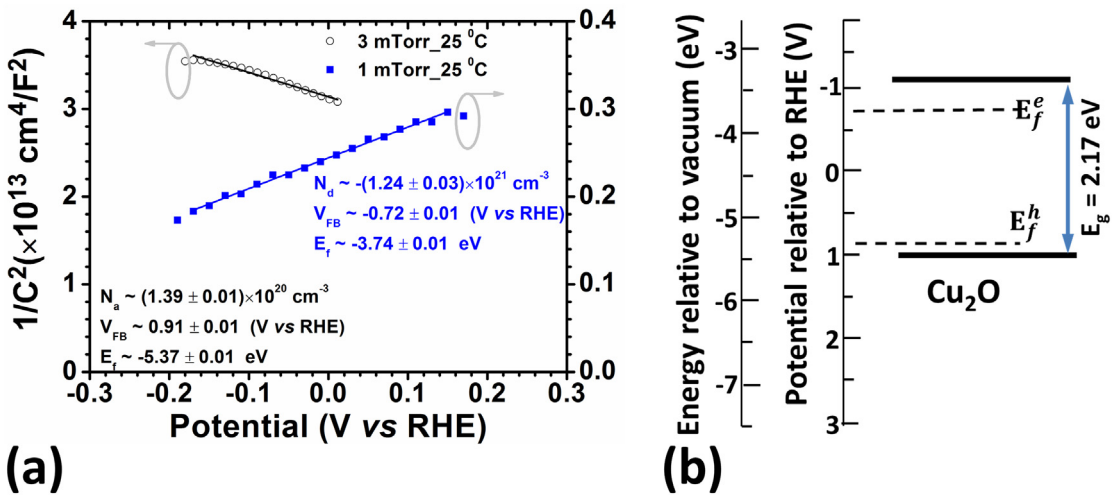

Fig. 7. (a) Mott-Schottky plots of Cu_2O thin films grow on ITO using 1 mTorr_25 °C and 3 mTorr_25 °C deposition conditions showing n-type and p-type conductivity respectively. The estimated carrier concentration, Flat band potential (V_{FB}) and quasi Fermi level energy (E_f^x; where $x = e$ or h) for donor and acceptor states are also shown in the inset. (b) An approximate band diagram of Cu_2O grown at low O_{2pp} and T_{sub} by PLD.

material for detail of the calculations). The high level of N_a, is consistent with low resistivity (few mΩ.cm), and low Hall mobilities (μ_H) ~1.03–4.78 cm^2/V.s and could be attributed to the scattering of holes at the grain boundaries of these RT-grown nanocrystalline films.

In contrast, the samples grown at 1 mTorr_ 25 °C(RT) exhibited an n-type conductivity with high level of donor concentrations (N_d) ~ -3.47×10^{21} cm^{-3} ($\mu_H \sim 0.85 \pm 0.01$ cm^2/V.s) and ~ -1.24×10^{21} cm^{-3} obtained from Hall coefficient measurements and M-S analyses respectively. The effective density of states ($D(E_f)$) for this sample is 1.05×10^{20} $(eV)^{-1}$ cm^{-3} and is slightly lower when compared to p-type RT-grown samples. However, such high level of carrier concentrations may contribute to its exceptionally low resistivity of ~3 mΩ·cm. The optical bandgap (~1.76 eV) of this n-type sample suggests that the donor level may be shallow. In the literature, the Fermi level of donor and acceptor levels for intrinsic Cu_2O is rarely reported ([9,22] and refs. therein). An approximate band diagram of a PLD-grown Cu_2O thin film electrode is shown in Fig. 7b using electrochemical M-S plot and UV-VIS-NIR optical data to demonstrate the quasi Fermi level energy of E_f^e(~0.28 eV below CBM) and E_f^h (~0.13 eV above VBM) for donor and acceptor states respectively. The Fermi level is estimated from Flat band potentials −0.72 V vs RHE (Fermi energy with respect to vacuum, $E_f = -3.73$ eV) and + 0.91 V vs RHE ($E_f = -5.37$ eV) respectively for n- and p-type Cu_2O/ITO electrodes using a similar approach as described in ref. [9]. The distinct positive- and negative-slope seen in M-S plots in Fig. 7a confirms the n- and p-type conductivity of Cu_2O/ITO electrodes and as seen in Fig. 7b the donor level is obviously located in more positive potentials than the acceptor level for Cu_2O which corroborate the reported results [9,24]. The estimated E_f^e ~0.28 eV below the conduction band minimum (CBM) is considerably shallower than the results of Garuthara et al. (~0.38 eV) [47] and E_f^h ~0.13 eV above the valence band maximum (VBM) which is slightly small compared to ~0.22 eV for V_{cu} and ~ 0.47 eV for $V_{cu,split}$ [22].

The low resistivity (ρ ~ 3 mΩ·cm) of n-type Cu_2O thin films grown by PLD is yet at least ~3 orders of magnitude above the resistivity of thermally evaporated metallic Cu (3.5 μΩ·cm) and Cu + Cu_2O (27 μΩ·cm) thin films reported by Figueiredo et al. [30]. Additionally, samples grown at 1 mTorr_ 25 °C(RT) are single phase Cu_2O, this is evident from both XRD (Fig. 2a) and TEM (Fig. 1a) analyses and they are the most oxygen deficient Cu_2O among the samples deposited in this study. Therefore, the origin of n-type conductivity in these PLD films is presumably due to the electron generating predominant oxygen vacancy (V_o) at the vicinity of Cu/Cu_2O phase boundary [23,39]. The single phase n-type Cu_2O deposited by electrodeposition with N_d as high as ~10^{20} cm^{-3} [15] has repeatedly been appeared in the literature, but single phase n-type Cu_2O deposited by PLD is rarely reported. Recently, Xu et al. [11] reported PLD grown phase pure Cu_2O using $O_{2pp} = 0.09$ Pa at $T_{sub} = 600$ °C with p-type conductivity and they were able to convert them into n-type Cu_2O via post-deposition N_2 plasma treatment. However, in our study the slight increase of O_{2pp} from 1 to 2 mTorr or more in the PLD chamber yielded p-type Cu_2O films suggesting that n-type Cu_2O can only be stabilized in a narrow range of $O_{2pp} \leq$ 1mTorr. Our findings for RT-grown samples suggest that critical regulation of low level O_{2pp} helps achieving single phase Cu_2O with tunable optical band gap ($E_g = 1.76$–2.15 eV) and type of conductivity with appreciable Hall mobilities (μ_H ~ 0.85–4.78 cm^2/V.s). Compared to results reported by Xu et al. this is important for synthesizing diverse optoelectronic device with low thermal budget [3,45] including p-n Cu_2O based homojunctions [7,9,12,14,24].

Table 1
Optical and Electrical properties of single phase Cu_2O and CuO thin films deposited with low O_{2pp} content during growth.

Growth condition (T_{sub}–O_{2pp})	Band gap (eV) ± 0.01	Thickness (nm) (VASE/SEM)	Resistivity (Ω·cm)	Carrier density (cm^{-3}) [Hall effect meas.]	Hall mobility (cm^2/V·s) ±0.01	Carrier density (cm^{-3}) [EIS meas.]
25_1	1.76	556 ± 21	2.12×10^{-3}	-3.47×10^{21}	0.85	$-(1.24 \pm 0.03) \times 10^{21}$
25_2	1.80	562 ± 4	8.71×10^{-3}	6.97×10^{20}	1.03	-
25_3	2.00	615 ± 25	24.00×10^{-3}	5.45×10^{19}	4.78	$(1.39 \pm 0.01) \times 10^{20}$
200_2	1.90	510 ± 7	49.28×10^{3}	5.71×10^{12}	22.21	-
200_3	2.00	585 ± 7	9.25×10^{3}	5.02×10^{13}	13.45	-
Ann. S1(CuO)	1.50	Assumed ~500	12.2 ± 0.7	-3.42×10^{17}	1.50	-

It is conspicuous that estimated acceptor concentrations in RT-grown p-Type Cu_2O samples are also high ($N_a \sim 6 \times 10^{19-20}$ cm^{-3}) in our observations (see Table 1 and Fig. 7). This is consistent with other recent reports. Theoretical studies reported by Raebiger et al. [16] suggest that the dominant defect V_{Cu} can be above 10^{21} cm^{-3} in concentrations, both in Cu-rich (oxygen poor) and Cu-poor(oxygen rich) growth conditions, to produce a p-type conductivity. Recent experimental works conducted by Zhang et al. [48] reported hole concentrations in the range 5.81×10^{18}–2.17×10^{21} cm^{-3} for sputtered Cu_2O thin films grown at room temperatures. Chen et al. [49] also reported that hole concentrations could be as high as 1.5×10^{21} cm^{-3}.

The PLD sample (S1) annealed at 550 °C in air for 1 h is single phase CuO and showed n-type conductivity with carrier concentration ~ 3.47×10^{17} cm^{-3} and mobility ~1.5 cm^2/V.s and is consistent with reported results [31]. The n-type conductivity of CuO can be understood as follows. PLD grown Cu_2O thin films with high O_{2pp} are copper deficient p-type semiconductors where the type of conductivity arises from the copper vacancies can be described by following equation:

$$½\ O_2 \leftrightarrow O_o + 2V_{Cu}^{-} + 2\ h^{+} \quad (1)$$

where, O_O - oxygen in regular positions of the lattice, V_{Cu}^{-} - metal vacancies, and h^+- holes. Due to annealing of p-type Cu_2O in air, more and more oxygen species are escaped from the Cu_2O matrix and generate more Cu^{2+} at the expense of Cu^{1+} in the films (this recrystallizes to a CuO phase) leading to the creation of an electron-generating oxygen vacancy (V_o^{+2}) according to the following equation:

$$O \leftrightarrow ½\ O_2 + V_o^{+2} + 2e^{-} \quad (2)$$

where, V_o^{+2} - oxygen vacancies, and e^- - electrons. As shown in Eq. (2), evolution of oxygen is accompanied by the formation of oxygen vacancies (with effective positive charge) and electrons that determine n-type of conductivity.

As a proof-of-concept, solid p-n junctions were fabricated with FTO/n-ZnO/p-Cu_2O/Au and p-Si(111)/n-Cu_2O structures. Their stable current-voltage characteristic curves suggest that p-n junctions were formed successfully, albeit with poor photovoltaic performance. These results are summarized and discussed in the supplementary materials (see Figs. S12–S14).

4. Conclusions

Single phase n- and p-type Cu_2O thin films were grown on quartz glass and other substrates (ITO, NaCl(100), and p-Si(111)) by a PLD technique and the influence of substrate temperatures and oxygen pressure (O_{2pp}) on the films properties were explored systematically. Thin films grown at 25 °C(RT) and 200 °C(HT) substrate temperatures are single phase Cu_2O with (200) and (111) texture respectively and their texturing is found to be increasing with the increasing oxygen content in the 2 mTorr ≤ O_{2pp} ≤ 5 mTorr PLD ambient. The optical bandgaps and electrical resistivities of RT-grown Cu_2O thin films were found to be tunable in the range 1.76 eV–2.15 eV and 3 mΩ·cm – 38 kΩ·cm respectively and both properties were found to be consistently increasing from low to higher values with increasing O_{2pp} due to more stoichiometric Cu(I) phase formation. Critical regulations of low level O_{2pp} during the growth process helps achieving both n- and p-type Cu_2O with appreciable Hall mobilities (μ_H ~ 0.85–4.78 cm^2/V.s). The as-grown p- and n-type Cu_2O showed promising rectification in solid junctions with n-ZnO and p-Si electrodes respectively. The findings reported here suggest that critical regulations of PLD growth conditions help achieve single phase Cu_2O growth with tunable electronic properties desirable for diverse optoelectronic applications.

CRediT authorship contribution statement

Syed Farid Uddin Farhad: Conceptualization, Investigation, Writing - original draft, Writing - review & editing. **David Cherns:** Conceptualization, Writing - review & editing. **James A. Smith:** Methodology, Writing - review & editing. **Neil A Fox:** Methodology, Writing - review & editing. **David J. Fermín:** Formal analysis, Writing - review & editing.

Declaration of competing interest

We declare that we have no conflict of interest.

Acknowledgments

S.F.U. Farhad acknowledges the financial help through BANGABANDHU fellowship, Ministry of Science and Technology, Government of Bangladesh to conduct this research. The authors are indebted to Professor Mike Ashfold FRS for allowing his PLD setup located at the Diamond laboratory, School of Chemistry, University of Bristol, UK during the Ph.D. studies. Special thanks are also due to Professor Walther Schawrzer, School of Physics, University of Bristol, UK for lending his Kiethley SMU2400 instrument in building a custom-made 4-point collinear probe resistivity measurement setup. D.J. Fermín acknowledges the support by the Engineering and Physical Sciences Research Council through the PVTEAM programme (EP/L017792/1). S.F.U Farhad also acknowledges the PV characterization support of the Energy Conversion and Storage Research (ECSR) section, Industrial Physics Division, BCSIR Labs, Dhaka, Bangladesh.

Data statement

All data provided in this manuscript and supporting materials are self-explanatory. There is no extra-data information which has been used in support of the arguments/result-explanations presented in the manuscript and supporting materials. However, the raw data used for generating the graph(s) in the manuscript and supporting materials will be made available on request. Notice, some explicitly related data could not be disclosed as they will be used for future scientific communication (s).

Appendix A. Supplementary data

Supplementary data to this article can be found online at https://doi.org/10.1016/j.matdes.2020.108848.

References

[1] H. Kim, S. Bae, D. Jeon, J. Ryu, Fully solution-processable Cu_2O–$BiVO_4$ photoelectrochemical cells for bias-free solar water splitting, Green Chem. 20 (2018) 3732–3742, https://doi.org/10.1039/c8gc00681d.

[2] Y.S. Zhi, P.G. Li, P.C. Wang, D.Y. Guo, Y.H. An, Z.P. Wu, X.L. Chu, J.Q. Shen, W.H. Tang, C.R. Li, Reversible transition between bipolar and unipolar resistive switching in Cu_2O/Ga_2O_3 binary oxide stacked layer, AIP Adv. 6 (2016), 015215. https://doi.org/10.1063/1.4941061.

[3] D. Muñoz-Rojas, M. Jordan, C. Yeoh, A.T. Marin, A. Kursumovic, L.A. Dunlop, D.C. Iza, A. Chen, H. Wang, J.L. MacManus Driscoll, Growth of ~5 $cm^2V^{-1}s^{-1}$ mobility, p-type copper (I) oxide (Cu_2O) films by fast atmospheric atomic layer deposition (AALD) at 225°C and below, AIP Adv. 2 (2012), 042179. https://doi.org/10.1063/1.4771681.

[4] H. Zhang, Q. Zhu, Y. Zhang, Y. Wang, L. Zhao, B. Yu, One-pot synthesis and hierarchical assembly of hollow Cu_2O microspheres with nanocrystals-composed porous multishell and their gas-sensing properties, Adv. Funct. Mater. 17 (2007) 2766–2771, https://doi.org/10.1002/adfm.200601146.

[5] K. Chen, S. Song, D. Xue, Faceted Cu_2O structures with enhanced Li-ion battery anode performances, CrystEngComm 17 (2015) 2110–2117, https://doi.org/10.1039/c4ce02340d.

[6] B.K. Meyer, A. Polity, D. Reppin, M. Becker, P. Hering, P.J. Klar, T. Sander, C. Reindl, J. Benz, M. Eickhoff, C. Heiliger, M. Heinemann, J. Bläsing, A. Krost, S. Shokovets, C. Müller, C. Ronning, Binary copper oxide semiconductors: from materials towards devices, Phys. Status Solidi B 249 (2012) 1487–1509, https://doi.org/10.1002/pssb.201248128.

[7] L.C. Olsen, F.W. Addis, W. Miller, Experimental and theoretical studies of Cu_2O solar cells, Solar Cells 7 (1982) 247–279, https://doi.org/10.1016/0379-6787(82)90050-3.

[8] A.E. Rakhshani, Preparation, characteristics and photovoltaic properties of cuprous oxide—a review, Solid State Electron. 29 (1986) 7–17, https://doi.org/10.1016/0038-1101(86)90191-7.

[9] C.M. McShane, K.S. Choi, Junction studies on electrochemically fabricated p-n Cu_2O homojunction solar cells for efficiency enhancement, Physical chemistry chemical physics: PCCP 14 (2012) 6112–6118, https://doi.org/10.1039/c2cp40502d.

[10] L. Xiong, S. Huang, X. Yang, M. Qiu, Z. Chen, Y. Yu, P-type and n-type Cu_2O semiconductor thin films: controllable preparation by simple solvothermal method and photoelectrochemical properties, Electrochim. Acta 56 (2011) 2735–2739, https://doi.org/10.1016/j.electacta.2010.12.054.

[11] M. Xu, X. Liu, W. Xu, H. Xu, X. Hao, X. Feng, Low resistivity phase-pure n-type Cu_2O films realized via post-deposition nitrogen plasma treatment, J. Alloys Compd. 769 (2018) 484–489, https://doi.org/10.1016/j.jallcom.2018.08.048.

[12] R.P. Wijesundera, L.K.A.D.D.S. Gunawardhana, W. Siripala, Electrodeposited Cu_2O homojunction solar cells: fabrication of a cell of high short circuit photocurrent, Sol. Energy Mater. Sol. Cells 157 (2016) 881–886, https://doi.org/10.1016/j.solmat.2016.07.005.

[13] J. Han, J. Chang, R. Wei, X. Ning, J. Li, Z. Li, H. Guo, Y. Yang, Mechanistic investigation on tuning the conductivity type of cuprous oxide (Cu_2O) thin films via deposition potential, Int. J. Hydrog. Energy 43 (2018) 13764–13777, https://doi.org/10.1016/j.ijhydene.2018.02.121.

[14] K. Han, M. Tao, Electrochemically deposited p–n homojunction cuprous oxide solar cells, Sol. Energy Mater. Sol. Cells 93 (2009) 153–157, https://doi.org/10.1016/j.solmat.2008.09.023.

[15] P. Wang, H. Wu, Y. Tang, R. Amal, Y.H. Ng, Electrodeposited Cu_2O as Photoelectrodes with controllable conductivity type for solar energy conversion, J. Phys. Chem. C 119 (2015) 26275–26282, https://doi.org/10.1021/acs.jpcc.5b07276.

[16] H. Raebiger, S. Lany, A. Zunger, Origins of the p-type nature and cation deficiency in Cu_2O and related materials, Phys. Rev. B 76 (2007)https://doi.org/10.1103/PhysRevB.76.045209.

[17] L.Y. Isseroff, E.A. Carter, Electronic structure of pure and doped cuprous oxide with copper vacancies: suppression of trap states, Chem. Mater. 25 (2013) 253–265, https://doi.org/10.1021/cm3040278.

[18] K.P. Musselman, A. Marin, A. Wisnet, C. Scheu, J.L. MacManus-Driscoll, L. Schmidt-Mende, A novel buffering technique for aqueous processing of zinc oxide nanostructures and interfaces, and corresponding improvement of electrodeposited ZnO-Cu_2O photovoltaics, Adv. Funct. Mater. 21 (2011) 573–582, https://doi.org/10.1002/adfm.201001956.

[19] S.S. Wilson, J.P. Bosco, Y. Tolstova, D.O. Scanlon, G.W. Watson, H.A. Atwater, Interface stoichiometry control to improve device voltage and modify band alignment in ZnO/Cu_2O heterojunction solar cells, Energy Environ. Sci. 7 (2014) 3606–3610, https://doi.org/10.1039/c4ee01956c.

[20] M. Pavan, S. Rühle, A. Ginsburg, D.A. Keller, H.-N. Barad, P.M. Sberna, D. Nunes, R. Martins, A.Y. Anderson, A. Zaban, E. Fortunato, TiO_2/Cu_2O all-oxide heterojunction solar cells produced by spray pyrolysis, Sol. Energy Mater. Sol. Cells 132 (2015) 549–556, https://doi.org/10.1016/j.solmat.2014.10.005.

[21] K. Kardarian, D. Nunes, P. Maria Sberna, A. Ginsburg, D.A. Keller, J. Vaz Pinto, J. Deuermeier, A.Y. Anderson, A. Zaban, R. Martins, E. Fortunato, Effect of mg doping on Cu_2O thin films and their behavior on the TiO_2/Cu_2O heterojunction solar cells, Sol. Energy Mater. Sol. Cells 147 (2016) 27–36, https://doi.org/10.1016/j.solmat.2015.11.041.

[22] D.O. Scanlon, G.W. Watson, Undoped n-type Cu_2O: fact or fiction? The Journal of Physical Chemistry Letters 1 (2010) 2582–2585, https://doi.org/10.1021/jz100962n.

[23] L. Frazer, K.B. Chang, R.D. Schaller, K.R. Poeppelmeier, J.B. Ketterson, Vacancy relaxation in cuprous oxide ($Cu_{2-x}O_{1-y}$), J. Lumin. 183 (2017) 281–290, https://doi.org/10.1016/j.jlumin.2016.11.011.

[24] L.C.-K. Liau, Y.-C. Lin, Y.-J. Peng, Fabrication pathways of p–n Cu_2O Homojunction films by electrochemical deposition processing, J. Phys. Chem. C 117 (2013) 26426–26431, https://doi.org/10.1021/jp405715c.

[25] S.F.U. Farhad, R.F. Webster, D. Cherns, Electron microscopy and diffraction studies of pulsed laser deposited cuprous oxide thin films grown at low substrate temperatures, Materialia 3 (2018) 230–238, https://doi.org/10.1016/j.mtla.2018.08.032.

[26] X. Liu, M. Xu, X. Zhang, W. Wang, X. Feng, A. Song, Pulsed-laser-deposited, single-crystalline Cu_2O films with low resistivity achieved through manipulating the oxygen pressure, Appl. Surf. Sci. 435 (2018) 305–311, https://doi.org/10.1016/j.apsusc.2017.11.119.

[27] S.H. Wee, P.S. Huang, J.K. Lee, A. Goyal, Heteroepitaxial Cu_2O thin film solar cell on metallic substrates, Sci. Rep. 5 (2015), 16272. https://doi.org/10.1038/srep16272.

[28] S. Ishizuka, K. Akimoto, Control of the growth orientation and electrical properties of polycrystalline Cu_2O thin films by group-IV elements doping, Appl. Phys. Lett. 85 (2004) 4920, https://doi.org/10.1063/1.1827352.

[29] S. Nandy, R. Thapa, M. Kumar, T. Som, N. Bundaleski, O.M.N.D. Teodoro, R. Martins, E. Fortunato, Efficient field emission from vertically aligned $Cu_2O_{1-\delta}$(111) nanostructure influenced by oxygen vacancy, Adv. Funct. Mater. 25 (2015) 947–956, https://doi.org/10.1002/adfm.201402910.

[30] V. Figueiredo, E. Elangovan, G. Gonçalves, P. Barquinha, L. Pereira, N. Franco, E. Alves, R. Martins, E. Fortunato, Effect of post-annealing on the properties of copper oxide thin films obtained from the oxidation of evaporated metallic copper, Appl. Surf. Sci. 254 (2008) 3949–3954, https://doi.org/10.1016/j.apsusc.2007.12.019.

[31] X. Hu, F. Gao, Y. Xiang, H. Wu, X. Zheng, J. Jiang, J. Li, H. Yang, S. Liu, Influence of oxygen pressure on the structural and electrical properties of CuO thin films prepared by pulsed laser deposition, Mater. Lett. 176 (2016) 282–284, https://doi.org/10.1016/j.matlet.2016.04.055.

[32] N. Gupta, R. Singh, F. Wu, J. Narayan, C. McMillen, G.F. Alapatt, K.F. Poole, S.-J. Hwu, D. Sulejmanovic, M. Young, G. Teeter, H.S. Ullal, Deposition and characterization of nanostructured Cu_2O thin-film for potential photovoltaic applications, J. Mater. Res. 28 (2013) 1740–1746, https://doi.org/10.1557/jmr.2013.150.

[33] A. Paracchino, J.C. Brauer, J.-E. Moser, E. Thimsen, M. Graetzel, Synthesis and characterization of high-Photoactivity electrodeposited Cu_2O solar absorber by Photoelectrochemistry and ultrafast spectroscopy, J. Phys. Chem. C 116 (2012) 7341–7350, https://doi.org/10.1021/jp301176y.

[34] S.F.U. Farhad, M.M. Hossain, N.I. Tanvir, S. Islam, Texture and bandgap tuning of phase pure Cu_2O thin films grown by a simple Potentiostatic electrodeposition technique, ECS Meeting Abstracts MA2020-01 (2020) 1212, https://doi.org/10.1149/ma2020-01191212mtgabs.

[35] S.F.U. Farhad, M.A. Hossain, N.I. Tanvir, R. Akter, M.A.M. Patwary, M. Shahjahan, M.A. Rahman, Structural, optical, electrical, and photoelectrochemical properties of cuprous oxide thin films grown by modified SILAR method, Mater. Sci. Semicond. Process. 95 (2019) 68–75, https://doi.org/10.1016/j.mssp.2019.02.014.

[36] M.Y. Ghotbi, Z. Rahmati, Nanostructured copper and copper oxide thin films fabricated by hydrothermal treatment of copper hydroxide nitrate, Mater. Des. 85 (2015) 719–723, https://doi.org/10.1016/j.matdes.2015.07.081.

[37] S.F.U. Farhad, Copper oxide thin films grown by pulsed laser deposition for photovoltaic applications, School of Physics, University of Bristol, UK January 2016, p. 222https://ethos.bl.uk/OrderDetails.do?uin=uk.bl.ethos.691178.

[38] K. Wang, W. Gao, H.W. Zheng, F.Z. Li, M.S. Zhu, G. Yang, G.T. Yue, Y.K. Liu, R.K. Zheng, Heteroepitaxial growth of Cu_2O films on Nb-$SrTiO_3$ substrates and their photovoltaic properties, Ceram. Int. 43 (2017) 16232–16237, https://doi.org/10.1016/j.ceramint.2017.08.205.

[39] O. Porat, I. Riess, Defect chemistry of $Cu_{2-y}O$ at elevated temperatures. Part II: electrical conductivity, thermoelectric power and charged point defects, Solid State Ionics 81 (1995)https://doi.org/10.1016/0167-2738(95)00169-7.

[40] Y. Wang, P. Miska, D. Pilloud, D. Horwat, F. Mücklich, J.F. Pierson, Transmittance enhancement and optical band gap widening of Cu_2O thin films after air annealing, J. Appl. Phys. 115 (2014), 073505. https://doi.org/10.1063/1.4865957.

[41] Syed Farid Uddin Farhad, David Cherns, Structural, optical and electrical properties of nanocrystalline Cu_2O thin films grown by pulsed laser deposition, Paper# 9AM-J8.30 Abstract book document# 1868681, MRS Spring Meeting and Exhibition, Material Research Society (MRS), San Francisco, California, USA, 2014https://doi.org/10.17632/whksg7scsx.1.

[42] L. Debbichi, M.C. Marco de Lucas, J.F. Pierson, P. Krüger, Vibrational properties of CuO and Cu_4O_3 from first-principles calculations, and Raman and infrared spectroscopy, J. Phys. Chem. C 116 (2012) 10232–10237, https://doi.org/10.1021/jp303096m.

[43] S.F.U. Farhad, N.I. Tanvir, M.S. Bashar, M.S. Hossain, M. Sultana, N. Khatun, Facile synthesis of oriented zinc oxide seed layer for the hydrothermal growth of zinc oxide nanorods, Bangladesh Journal of Scientific and Industrial Research 53 (2018) 233, https://doi.org/10.3329/bjsir.v53i4.39186.

[44] S.B. Ogale, P.G. Bilurkar, N. Mate, S.M. Kanetkar, N. Parikh, B. Patnaik, Deposition of copper oxide thin films on different substrates by pulsed excimer laser ablation, J. Appl. Phys. 72 (1992) 3765–3769, https://doi.org/10.1063/1.352271.

[45] A. Subramaniyan, J.D. Perkins, R.P. O'Hayre, S. Lany, V. Stevanovic, D.S. Ginley, A. Zakutayev, Non-equilibrium deposition of phase pure Cu_2O thin films at reduced growth temperature, APL Materials 2 (2014), 022105. https://doi.org/10.1063/1.4865457.

[46] B. Bera, A. Chakraborty, T. Kar, P. Leuaa, M. Neergat, Density of states, carrier concentration, and flat band potential derived from electrochemical impedance measurements of N-doped carbon and their influence on Electrocatalysis of oxygen reduction reaction, J. Phys. Chem. C 121 (2017) 20850–20856, https://doi.org/10.1021/acs.jpcc.7b06735.

[47] R. Garuthara, W. Siripala, Photoluminescence characterization of polycrystalline n-type Cu_2O films, J. Lumin. 121 (2006) 173–178, https://doi.org/10.1016/j.jlumin.2005.11.010.

[48] L. Zhang, L. McMillon, J. McNatt, Gas-dependent bandgap and electrical conductivity of Cu_2O thin films, Sol. Energy Mater. Sol. Cells 108 (2013) 230–234, https://doi.org/10.1016/j.solmat.2012.05.010.

[49] X. Chen, D. Parker, M.-H. Du, D.J. Singh, Potential thermoelectric performance of hole-doped Cu_2O, New J. Phys. 15 (2013), 043029. https://doi.org/10.1088/1367-2630/15/4/043029.